

# Label Anything: Multi-Class Few-Shot Semantic Segmentation with Visual Prompts

Pasquale De Marinis<sup>1</sup>, Nicola Fanelli<sup>1</sup>, Raffaele Scaringi<sup>1</sup>, Emanuele Colonna<sup>1</sup>, Giuseppe Fiameni<sup>2</sup>, Gennaro Vessio<sup>1</sup>, and Giovanna Castellano<sup>1</sup>

<sup>1</sup> Department of Computer Science, University of Bari Aldo Moro, Italy  
name.surname@uniba.it

<sup>2</sup> NVIDIA AI Technology Center, Bologna, Italy  
gfiameni@nvidia.com

**Abstract.** We present Label Anything, an innovative neural network architecture designed for few-shot semantic segmentation (FSS) that demonstrates remarkable generalizability across multiple classes with minimal examples required per class. Diverging from traditional FSS methods that predominantly rely on masks for annotating support images, Label Anything introduces varied visual prompts—points, bounding boxes, and masks—thereby enhancing the framework’s versatility and adaptability. Unique to our approach, Label Anything is engineered for end-to-end training across multi-class FSS scenarios, efficiently learning from diverse support set configurations without retraining. This approach enables a “universal” application to various FSS challenges, ranging from 1-way 1-shot to complex  $N$ -way  $K$ -shot configurations while remaining agnostic to the specific number of class examples. This innovative training strategy reduces computational requirements and substantially improves the model’s adaptability and generalization across diverse segmentation tasks. Our comprehensive experimental validation, particularly achieving state-of-the-art results on the COCO-20<sup>i</sup> benchmark, underscores Label Anything’s robust generalization and flexibility. The source code is publicly available at: <https://github.com/pasqualedem/LabelAnything>.

**Keywords:** Few-Shot Semantic Segmentation, Visual Prompts, Multi-Class Segmentation, Class Prototypes, Deep Learning Architectures

## 1 Introduction

The advancement of semantic segmentation has been closely linked to the availability of extensive labeled datasets, which often pose a significant challenge in deploying these systems for real-world applications. Typically, models trained on such datasets excel at recognizing and classifying objects they were trained on but falter when encountering new concepts or domains, thus limiting their

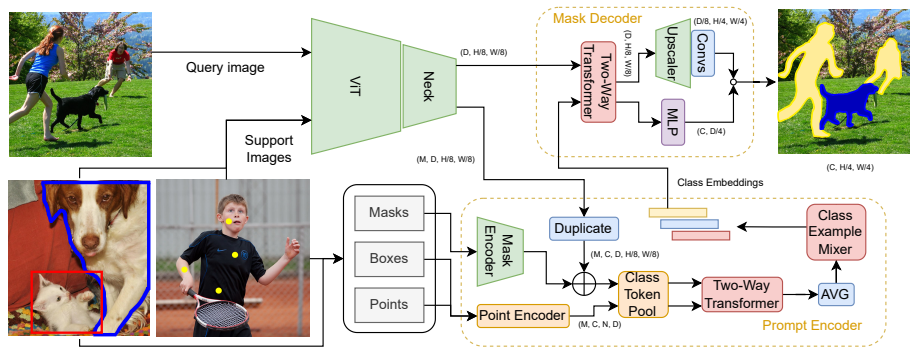


**Fig. 1:** Overview of the proposed framework, illustrating the workflow for a 1-shot scenario involving three classes, two support images, and all three types of prompts. Label Anything leverages a pre-trained ViT to derive image features. Prompts are fed into the Prompt Encoder, which generates a distinct prototype for each class. Subsequently, these prototypes inform the Mask Decoder, facilitating accurate pixel classification across the query image.

practical utility. Segmenting objects from previously unseen classes with few or no labeled examples remains a pivotal challenge in computer vision.

Few-shot semantic segmentation (FSS) has recently gained attention as the task of segmenting a query image based on a limited set of examples [26]. While the majority of research in FSS has concentrated on binary segmentation tasks (distinguishing background from foreground), there has been limited exploration of methods capable of segmenting multiple classes simultaneously, a step toward more flexible and *domain-agnostic* segmentation [4, 13, 14, 30, 33, 42]. Furthermore, aside from an initial exploration by Rakelly et al. [24], which considered coordinates as prompts, the field has predominantly focused on mask annotations as the sole input type. This underscores the growing need to support diverse input annotations, reducing reliance on extensive human annotation and facilitating smoother integration with other models, such as object detectors that generate bounding boxes.

This work presents Label Anything (LA), a novel deep neural network architecture designed for multi-prompt, multi-class FSS. Our method embraces a *prototype-based* learning paradigm, leveraging diverse visual prompts—points, bounding boxes, and masks—to create a highly flexible and generalizable framework (Fig. 1 illustrates our approach). This innovation not only addresses the challenge of segmenting objects from unseen classes with limited examples but also significantly reduces the annotation burden.

Building upon Segment Anything’s innovative use of diverse prompts for segmentation [9], our method significantly enriches FSS by enhancing support set adaptability and extending the framework into multi-class challenges. Unlike traditional approaches that focus on binary segmentation and adhere to strict class example limits, LA supports various prompt types and a flexible number

of class examples per support set. This flexibility allows for capturing complex inter-class relationships from a single image, improving segmentation precision. Moreover, LA’s architecture is designed to learn from different support set configurations and prompt types in a single training cycle, eliminating the need for retraining across different FSS scenarios. Such versatility ensures that LA can be applied across a wide range of domains, offering a comprehensive solution that moves beyond the constraints of conventional FSS models.

Our extensive experimental analysis on the well-known COCO-20<sup>i</sup> benchmark [22, 33] reveals that our model achieves state-of-the-art performance, setting a new standard in the field. The contributions of LA are not merely technical but also practical as we pave the way for more accessible and efficient semantic segmentation, especially in scenarios where annotation resources are scarce.

The rest of this paper is organized as follows. Section 2 reviews related work. Section 3 details our proposed approach. Section 4 evaluates our model’s performance. Section 5 concludes the paper with a summary of our findings and directions for future research.

## 2 Related Work

### 2.1 Few-Shot Semantic Segmentation

Semantic segmentation, which involves assigning a class label to each pixel in an image, is a fundamental task in computer vision. The introduction of Convolutional Neural Networks (CNNs), with pioneering architectures like the Fully-Convolutional Network [17] and U-Net [25], was pivotal in pushing the field forward. These architectural innovations laid the foundation for numerous subsequent methods, each tailored to address specific challenges (e.g., [3, 23]).

Building upon few-shot learning principles [6, 28, 29, 32], few-shot semantic segmentation has developed as a significant extension of semantic segmentation to achieve high accuracy with minimal reliance on large, annotated datasets. FSS involves per-pixel classification in a query image, guided by a “support set” typically comprising a small number of images and their corresponding mask annotations. This task hinges on the model’s ability to leverage support set information for accurate segmentation.

Early attempts in FSS utilized CNNs to synthesize support set information. This information was integrated into the segmentation process by modifying weights and biases or merging it with query image features [24, 26]. This foundational work laid the groundwork for more sophisticated approaches broadly categorized into *prototype*-based and *affinity*-based learning. Prototype-based methods focus on deriving one or several representative prototypes for the concept to be segmented, applying these to the query image through distance metrics or decoder networks [4, 10, 14, 15, 33, 39, 42, 43]. In contrast, affinity learning approaches delve into the pixel-wise relationships between support and query features [1, 21, 27, 35, 40]. Nearly all methods in FSS leverage the extensive feature pyramids extracted by CNNs for query and support images. Only recent works

such as FPTrans [41] have begun to explore the use of the Vision Transformer (ViT) [5] as the encoder.

In recent years, considerable interest has been shown in FSS. However, most research has focused on a binary paradigm, where images are segmented based on a single concept specified by the support set. The binary (single-way) and multi-class FSS settings present distinct challenges. Binary classification models struggle to adapt to multi-class scenarios without a significant drop in performance, highlighting the need for specialized solutions.

A limited number of studies have ventured into the complex domain of multi-class FSS [4, 13, 14, 30, 33, 42]. This involves enabling the support set to introduce multiple classes for segmentation, requiring the model to distinguish between  $N$  predefined classes in the query image, a departure from the more straightforward foreground-background dichotomy. Multi-class FSS typically adopts an  $N$ -way  $K$ -shot framework, entailing  $N$  classes within the support set and  $K$  instances per class. This approach, geared towards segmenting multiple classes, invariably relies on a prototype-based model architecture to encapsulate and convey class-specific information throughout the network. For example, MFNet [42] leverages Masked Global Pooling alongside attention mechanisms to generate class prototypes that integrate with query image features for segmentation.

It is crucial to recognize that the efficacy of multi-way methodologies is contingent upon predefined  $N$  and  $K$  values, necessitating their specification prior to training—a constraint that also influences many single-way models in terms of the number of examples per segmented concept.

## 2.2 Promptable Segmentation

Integrating *prompt*-based learning, inspired by its success in natural language processing, into computer vision introduced a novel paradigm. In particular, a significant breakthrough came from the Segment Anything model (SAM), introduced by Kirillov et al. [9]. This innovation harnesses an interactive, prompt-guided vision framework, representing a pivotal moment reminiscent of the GPT series but in computer vision. SAM has been trained on a vast dataset comprising over 1 billion masks extracted from 11 million images, employing a “promptable” segmentation task. This innovative approach equips SAM with the unique capability for robust zero-shot generalization, enabling it to excel in a wide range of tasks such as edge detection and instance segmentation.

In recent times, the research community has been prolific in extending the capabilities of SAM and exploring its potential across diverse domains. These endeavors have pushed the boundaries of what SAM can accomplish and have successfully applied it to a wide range of tasks, including medical image analysis [20], image inpainting [37], and image editing [36]. Recent innovations like SegGPT [34] and SEEM [44] have extended the use of prompts to guide predictions, exploring the integration of textual and audio prompts to enhance model performance across diverse tasks.

However, despite these advancements, there remains a gap in applying these models to FSS, especially in classifying objects into previously unseen classes



based on a limited number of annotated examples. While models like SegGPT show promise in FSS scenarios, their generalization capabilities are often attributed to the vast datasets used for training rather than an inherent ability to leverage support set information effectively. Furthermore, apart from an early exploration by Rakelly et al. [24], research in FSS has scarcely investigated the use of diverse annotations within support sets—such as points or bounding boxes—as alternatives to traditional mask prompts, leaving a substantial area of FSS largely unexplored.

### 2.3 Our Contribution

Our work seeks to bridge the gaps in the literature using various visual prompts to guide the FSS task. Drawing from cutting-edge prompt-based segmentation techniques, LA innovatively employs an array of prompt types within the FSS framework. Our novel end-to-end neural network architecture is also designed for multi-class FSS, enhancing the versatility of forming support sets, crucial for effective FSS. Moving beyond the conventional focus on binary FSS, which mainly leverages affinity-based methods, our work proposes a prototype-based architecture. This design choice aligns with the efficiency and coherence demands of multi-way scenarios and addresses the limitations imposed by the significant memory requirements of affinity-based approaches in  $N$ -way  $K$ -shot setups. Taking cues from successful 1-way  $K$ -shot models (e.g., [21, 27, 31, 38]), which adapt to generic  $K$ -shot scenarios post-training, our method expands this approach to accommodate multi-class contexts. We train our model once, enabling it to seamlessly adapt to various FSS benchmarks, including 1-way 1-shot and  $N$ -way  $K$ -shot configurations, without imposing any constraints on the number of examples ( $K$ ) per class. This approach affords unparalleled flexibility, allowing the model to interpret support sets comprising any number of images and annotations, irrespective of class or prompt type. Such enhancements inherently reduce computational demands and significantly boost the model’s versatility and robustness in diverse FSS scenarios.

## 3 Label Anything

We aim to develop a model capable of labeling any image across any class using a minimal set of prompts for each class. This approach does not prescribe a predefined number of prompts per class; instead, it mandates that the support set comprehensively covers all required classes.

### 3.1 Problem Formulation

We introduce the task of *multi-prompt, multi-way, few-shot* semantic segmentation. This involves classifying the pixels of a query image  $I_q$  into one of  $N + 1$  classes, with  $N$  denoting the number of foreground categories to be segmented. The  $N$  foreground concepts are learned using only a few annotated images. To

achieve this goal, we employ “episodic training” [32], which consists of training episodes involving a query image and a distinct support set.

Formally, our dataset is partitioned into two subsets: a training set  $\mathcal{D}_{train}$  and a test set  $\mathcal{D}_{test}$ . Crucially, we define two distinct sets of segmentation categories,  $\mathcal{C}_{seen}$  for training and  $\mathcal{C}_{unseen}$  for testing, ensuring  $\mathcal{C}_{seen} \cap \mathcal{C}_{unseen} = \emptyset$ . Annotations in  $\mathcal{D}_{train}$  utilize classes from  $\mathcal{C}_{seen}$ , whereas  $\mathcal{D}_{test}$  is evaluated on classes from  $\mathcal{C}_{unseen}$ , representing concepts not encountered during training to assess the model’s generalization capabilities in a few-shot setting.

Each training episode presents the model with a query and its corresponding ground truth  $(I_q, M_q)$ , where  $I_q$  is an RGB image of dimensions  $3 \times H \times W$  and  $M_q$  is a segmentation mask associating pixels of  $I_q$  with one of  $N + 1$  classes. The model receives a support set  $\mathcal{S} = \{(I_i, A_i)\}_{i=1}^L$  comprising  $L$  image-prompt annotation pairs to assist in classifying the query pixels. Each pair  $(I_i, A_i)$  is called a “shot”, with  $L$  usually being a small number. For instance, in multi-class FSS tasks,  $L$  is often determined as  $N \times K$ , with  $K$  indicating the number of examples, or shots, per class necessary for the model to learn about class  $n$ . Standard testing configurations on benchmark datasets typically involve setting  $N$  and  $K$  to values from the set  $\{1, 2, 5\}$ .

Our approach significantly extends the flexibility of FSS by allowing for multiple types of prompts—masks, points, and bounding boxes—within the support set. Unlike previous FSS methodologies, LA does not require the support set size  $L$  to match  $N \times K$  strictly, enabling variable numbers of shots per class. Additionally, LA permits a single image to serve as a support example for multiple classes without repetition, linking different class prompts to the same image, thus maximizing the exploitation of inter-class relationships within annotations.

In more detail, we have  $A_i = \{(M_{i,n}, P_{i,n}, B_{i,n})\}_{n=1}^N$  for each support set image, where  $M_{i,n}$  is a binary mask for class  $n$  in image  $i$ ,  $P_{i,n}$  represents point coordinates, and  $B_{i,n}$  denotes bounding boxes. The prompt type for class  $n$  in image  $i$  is randomly selected during training, with padding applied as necessary for absent classes or prompt types. Evaluation on  $\mathcal{D}_{test}$  involves support set annotations from  $\mathcal{C}_{unseen}$ , testing the model’s adaptability to new classes.

### 3.2 Model Architecture

Label Anything processes a query image  $I_q$  for segmentation alongside a support set  $\mathcal{S}$ , utilizing three core components in its architecture (refer to Fig. 1): the Image Encoder, the Prompt Encoder, and the Mask Decoder.

The Image Encoder leverages a pre-trained Vision Transformer, specifically ViT-B/16 [5] to process the query and support images. These images are transformed into feature maps  $F_q$  for the query and  $F_s$  for the support set, with dimension  $D_{ViT} \times H_d \times W_d$ , where  $H_d = H/x_p$  and  $W_d = W/x_p$  and  $x_p$  is the ViT patch size. Attached to ViT is a convolutional neck that processes the image features to reduce their dimensionality from  $D_{ViT} = 768$  to  $D = 512$ .

The Prompt Encoder is a key component of the LA architecture, designed to embody different types of prompts—masks, boxes, and points—from support images and effectively encapsulate this information. In its initial stage, the Prompt

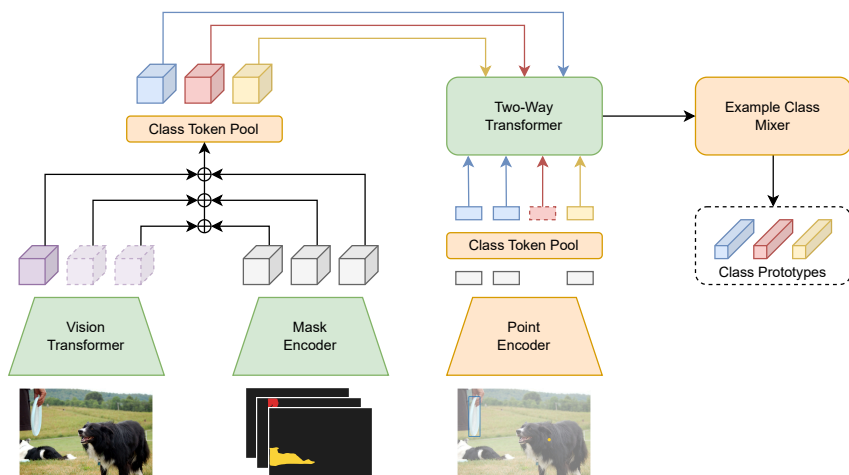


**Fig. 2:** Class prototype generation process. LA begins with extracting image features from a single support set example using ViT. This example might include multiple prompts related to different classes and types. A CNN-based Mask Encoder processes dense prompts (masks), while point coordinates and bounding boxes are transformed into embeddings via the Point Encoder, with bounding boxes treated as pairs of point embeddings. These processed prompts are then integrated with the image features. The Class Token Pool enriches dense and sparse embeddings with class information to infuse class-specific semantics. Subsequent two-way cross-attention between dense and sparse features yields class prototypes for each example.

Encoder processes these inputs to generate embeddings: masks are encoded using a CNN, resulting in dense embeddings ( $P_d$ ), while points and boxes are encoded through a Point Encoder, which uses Positional Embeddings to produce sparse embeddings for points and boxes ( $P_s$ ). Three different learnable embeddings are used, each corresponding to the three types of coordinate inputs (point prompt, box top-left corner, box bottom-right corner), which are then summed. To enable attention on various objects as dictated by sparse prompt features, a self-attention layer complemented by a residual connection is employed. The layer operates on an input dimensionality of  $BL \times NM \times D$ , signifying batch size ( $B$ ), number of examples ( $L$ ), classes ( $N$ ), prompts per class ( $M$ ), and feature size ( $D$ ), thereby facilitating independent example processing and attention to each prompt feature across both similar and different classes. We adopt the Token Pool strategy from Zhang et al. [41] to incorporate class-specific information using a trainable random Gaussian matrix sized  $R \times D$ , where  $R$  should be greater than the number of classes. At each step, a row is sampled from this matrix for each class and added to the sparse and dense features. Subsequently, dense embeddings are combined with the image features to highlight the featured object within the feature map. Merging sparse and dense embeddings in a

single feature map requires a Two-Way Transformer, similar to the mechanism in SAM [9]. This Transformer alternates attention between dense to sparse features and vice versa, according to:

$$P_s = \text{MultiHeadAttention}(P_s, P_d + PE, P_d + PE), \quad (1)$$

$$P_d = \text{MultiHeadAttention}(P_d + PE, P_s, P_s), \quad (2)$$

where  $PE$  denotes the positional encoding adjusted for dimensions  $(H, W)$ . This process ensures a comprehensive integration of prompt-based information, highlighting the relevance of each object within the feature map.

After processing sparse features, these features are eliminated, forcing the model to encapsulate all pertinent details within the dense features. A Global Average Pooling layer then condenses the spatial dimensions, generating a set of class-example embeddings  $E = \{E_{ni} \in \mathbb{R}^D | \forall n \in \mathcal{C}, \forall i \in \mathcal{S}\}$ . To facilitate the interchange of information across examples and classes, we introduce the Class Example Mixer block, which enables communication between different examples through a Transformer layer. The attention layer in it enables the embeddings of the same class  $n$  over different examples to be attended:

$$E_n = E_{n_1}, E_{n_2}, \dots, E_{n_L} \quad (3)$$

$$E_n = \text{MultiHeadAttention}(E_n, E_n, E_n) \quad (4)$$

Embeddings are averaged across examples to yield a singular prototype per class, compacting essential class information. Figure 2 shows a detailed view of the class prototype generation for a single support set example.

The Mask Decoder uses the class prototypes  $E_1, \dots, E_{|\mathcal{C}|}$  (or class-example prototypes at test time), and the query image features  $F_q$  to generate a segmentation mask for each class. This process begins with the Two-Way Transformer, which serves a role different from its Prompt Encoder function. Here, it aims to facilitate pattern matching between class prototypes and pixel locations within the query image by reciprocally attending to them, thus transferring relevant information for segmentation. Subsequently, the query features are upsampled to a resolution of  $(H/4, W/4)$ , and their dimensionality is reduced to  $D/8$  through a sequence of transposed convolutional layers. Concurrently, the class prototypes are dimensionally aligned to match the query features via an MLP, ensuring uniformity in representation. Following this, the modified query features  $F_q$  undergo further refinement through three  $3 \times 3$  spatial convolutional layers aimed at producing segmentation outputs that are not only smoother but also spatially coherent. The segmentation logits for each pixel and class are determined through a dot product operation, succinctly captured by the formula:

$$\text{Logit}_{xy,n} = F_{q_{xy}} \cdot E_n, \quad (5)$$

thereby computing the final segmentation masks.

### 3.3 Training Procedure

One of the primary objectives of this work is to enable our model to be trained *once* for application across arbitrary combinations of  $N$  and  $K$  during testing

and across various prompt inputs. To accomplish this, we introduce an innovative episodic training approach that optimizes resource utilization while accommodating diverse  $N$ ,  $K$ , and prompt-type configurations.

The procedure starts by defining potential batch configurations as  $(B, N, K)$ , where  $B$  represents the batch size, indicating the number of learning episodes per batch. The selection of  $B$  is tailored to the  $N$  and  $K$  parameters to ensure optimal GPU resource management using powers of 2, with  $B \times N \times K + B$  representing the aggregate image count per batch, including both support and query images. Each training batch is then constructed by randomly selecting a  $(B, N, K)$  tuple.

For every episode within a batch,  $N$  classes are randomly chosen from the set of seen classes,  $\mathcal{C}_{seen}$ . A coin flip probabilistic decision determines whether the query image should contain any or all of the  $N$  selected classes, adjusting  $N$  if a comprehensive query image is unavailable. This variability fosters episodes where the query image encompasses objects from all sampled classes and scenarios, necessitating the exclusion of certain support set classes during segmentation, thereby addressing a recognized bias in FSS research [8].

Subsequently,  $K$  support examples per class are sampled. We identify all annotations corresponding to the selected  $N$  classes within each chosen image, allowing multiple annotations per image. This flexibility ensures our model’s readiness for any  $L$  image-annotation pair configuration, where  $L$  may deviate from the strict  $N \times K$  formula.

Additionally, our training episodes are enriched by incorporating a random selection of prompt types for each instance annotation within the support set, enhancing the diversity of learning stimuli. For instances requiring point annotations, points are sampled proportionately to the instance’s mask area, tailoring the learning process to the specific needs of each episode and prompt type.

## 4 Experimental Evaluation

We evaluated LA across two distinct FSS tasks: 1-way 1-shot segmentation and  $N$ -way  $K$ -shot segmentation. Performance is reported as mean Intersection-over-Union (mIoU) across test classes.

### 4.1 Dataset and Validation

Our assessment was based on the COCO-20<sup>i</sup> dataset [22, 33], a predominant FSS benchmark sourced from the MS COCO dataset [12], to evaluate our model across both 1-way 1-shot and  $N$ -way  $K$ -shot segmentation tasks. COCO-20<sup>i</sup> amplifies the challenge by dividing its 80 classes into four distinct folds, each encompassing 20 classes. Employing cross-validation, we rotated classes within each fold as  $\mathcal{C}_{unseen}$ , contrasting with  $\mathcal{C}_{seen}$  for the remaining classes. This setup aligned  $\mathcal{D}_{train}$  and  $\mathcal{D}_{test}$  with the original dataset’s arrangement, ensuring our model faced novel images and classes during testing. Our model was fine-tuned in

a single iteration per cross-validation phase, highlighting our training strategy’s effectiveness.

To ensure a rigorous comparison with established benchmarks, especially in binary FSS contexts [21, 22], we adopted a consistent evaluation methodology, conducting tests over 1000 randomly chosen episodes, utilizing 5 distinct random seeds for each and averaging the outcomes. This procedure was replicated for  $N$ -way  $K$ -shot evaluations, aligning with methodologies from prominent studies [14, 33, 42]. Unless otherwise stated, we limited our prompt type to masks during tests for more accurate benchmarking, facilitating direct comparisons across different approaches and configurations.

## 4.2 Setting

We adopted a uniform input resolution of  $1024 \times 1024$  for query and support images, resizing images and applying padding to maintain the aspect ratio. Following the methodology proposed by Zhang et al. [41], we used the ViT-B/16 model [5], augmented with Segment Anything [9] pretraining and with its weights kept frozen, serving as our backbone. This configuration yielded a singular feature map per image. Class-specific masks were supplied at a refined resolution of  $256 \times 256$ , while points and bounding boxes were integrated into the model using normalized coordinates.

Moreover, for a fairer comparison with existing methods, we also employed the same ViT-B/16 architecture with the Masked Autoencoder (MAE) pre-training strategy [2]. The input size was  $480 \times 480$ , with the output feature map of dimension  $768 \times 30 \times 30$ . This pretraining strategy is preferred against the classical ImageNet classification pre-training as it retains the spatial features useful for segmentation.

Our training strategy optimized the focal loss [11], which addresses class imbalance by focusing on difficult-to-classify examples computed for a single training instance as:

$$\mathcal{L} = \frac{1}{N+1} \sum_n^{N+1} \left[ w_n \cdot (1 - e^{-l_{ce}(\hat{y}_n, y_n)})^\gamma \cdot l_{ce}(\hat{y}_n, y_n) \right], \quad (6)$$

where  $N + 1$  is the number of classes,  $w_n$  are class-specific weights,  $l_{ce}$  the cross-entropy loss, and  $\gamma$  the focusing parameter adjusting the emphasis on hard examples.

We used the AdamW optimizer [19] ( $\beta_1 = 0.9$ ,  $\beta_2 = 0.999$ ), complemented by a linear learning rate warmup [7] for 1000 iterations, followed by a step-wise cosine learning rate decay schedule [18]. The initial learning rate, after warmup, was  $1e-5$ . Our training followed the configurations outlined in Sec. 3.3, adopting batch size-number of classes-number of shots configurations such as (4, 1, 4), (2, 4, 2), (8, 1, 2), (4, 2, 2), (4, 4, 1), and (16, 1, 1), where the batch size refers to a single GPU. The model underwent training for 50 epochs, with the iteration count per epoch equivalent to the size of  $\mathcal{D}_{train}$ . A cap was placed on point samples at a maximum of 10 per instance to maintain efficiency. The architecture

Method	1-way 1-shot					1-way 5-shot				
	fold-0	fold-1	fold-2	fold-3	mean	fold-0	fold-1	fold-2	fold-3	mean
DCAMA [27]	<b>49.5</b>	<b>52.7</b>	<b>52.8</b>	<b>48.7</b>	<b>50.9</b>	<b>55.4</b>	<b>60.3</b>	<b>59.9</b>	<b>57.5</b>	<b>58.3</b>
FPTrans [40]	39.7	44.1	44.4	39.7	42.0	49.9	56.5	55.4	53.2	53.8
LA (MAE)	35.2	44.0	39.4	40.4	39.7	38.5	44.8	39.5	42.3	41.2
LA (SAM)	39.2	46.6	44.1	42.7	43.1	42.4	49.3	45.9	43.4	45.1

**Table 1:** Results for 1-way  $K$ -shot segmentation, benchmarking against leading transformer-based FSS methodologies. DCAMA [27] represents the peak in affinity learning-based segmentation, leveraging the hierarchical Vision Transformer Swin-B [16] as its foundation. Conversely, FPTrans [41] exemplifies top-tier performance in prototype-based segmentation, employing the ViT-B/16 [5] as its backbone.

totals 27 million learnable parameters, reflecting the model’s complexity and capacity for handling diverse FSS scenarios.

Training leveraged the Leonardo cluster’s resources, including 512GB of RAM and four NVIDIA A100-64GB GPUs, to support the computational demands, ensuring high-performance processing capabilities.

### 4.3 Results

In Table 1, we showcase the performance of LA on the COCO-20<sup>i</sup> benchmark, juxtaposing it with leading binary FSS methods. Our model achieved state-of-the-art results among prototype-based approaches, notably surpassing FPTrans [41] in the 1-shot setting. However, DCAMA [27], an affinity-based method, exceeds our performance by comparing each pixel in the query image against every pixel in the support images, leveraging features from multiple backbone levels. Given its detailed pixel-wise comparison strategy, DCAMA’s superior performance was anticipated. Despite this, affinity-based methods face scalability challenges, particularly in  $N$ -way  $K$ -shot scenarios, as the number of necessary comparisons increases quadratically with the image count and, by extension, with the class count. This limitation underscores the practical advantages of prototype-based models like LA for complex segmentation tasks involving multiple classes and shots.

Indeed, Table 2 presents the performance of LA and several other state-of-the-art methods on the 2-way  $K$ -shot segmentation task, as evaluated on the COCO-20<sup>i</sup> benchmark. LA demonstrates superior performance across all four folds, excelling in the more challenging 2-way 1-shot and 2-way 5-shot scenarios, achieving the highest mIoU scores. Notably, LA surpassed MFNet [42], previously regarded as the leading method, especially in folds 1, 2, and 3, underscoring its superior ability to handle multi-class segmentation tasks with limited examples. Other methods show competitive but lower performance compared to LA, highlighting the effectiveness of our approach in leveraging diverse visual prompts and an end-to-end training strategy.

Method	2-way 1-shot					5-way 1-shot				
	fold-0	fold-1	fold-2	fold-3	mean	fold-0	fold-1	fold-2	fold-3	mean
PANet [33]	25.7	16.1	16.2	13.8	18.0	22.1	16.0	14.1	11.9	16.0
PPNet(w/o U) [14]	29.0	19.4	16.5	14.2	19.8	24.3	16.8	14.3	12.8	17.1
PPNet [14]	29.8	19.7	17.0	15.1	20.4	25.6	17.3	15.5	13.4	18.0
DENet [13]	30.3	20.5	16.7	15.3	20.7	27.0	17.9	14.6	14.0	18.4
MFNet [42]	<b>35.3</b>	24.0	18.4	18.7	24.1	<b>29.7</b>	21.2	15.4	17.1	20.9
LA (MAE)	30.6	33.6	32.2	31.2	31.9	21.1	25.1	26.4	27.5	25.1
LA (SAM)	31.0	<b>38.2</b>	<b>34.7</b>	<b>34.5</b>	<b>34.6</b>	24.2	<b>27.5</b>	<b>29.6</b>	<b>29.7</b>	<b>27.7</b>

**Table 2:** Performance on 2-way / 5-way 1-shot segmentation benchmarked with contemporaneous methods as re-evaluated in the MFNet study [42]. Comparisons are made using mIoU percentages, specifically focusing on foreground classes. Misclassifications within these classes are considered under false positive and false negative categories for the respective classes; a measurement approach denoted as mIoU\* in the MFNet analysis.

Method	1-way	2-way	3-way	4-way	5-way	10-way	15-way	20-way
DCAMA	<b>50.9</b>	31.7	24.2	21.1	16.7	10.8	6.5	4.7
LA (MAE)	39.7	31.9	28.6	26.5	25.1	20.7	15.0	10.8
LA (SAM)	43.1	<b>34.6</b>	<b>31.7</b>	<b>29.6</b>	<b>27.7</b>	<b>23.6</b>	<b>16.9</b>	<b>13.7</b>

**Table 3:** Average mIoU results for  $N$ -way 1-shot on COCO-20<sup>i</sup>.

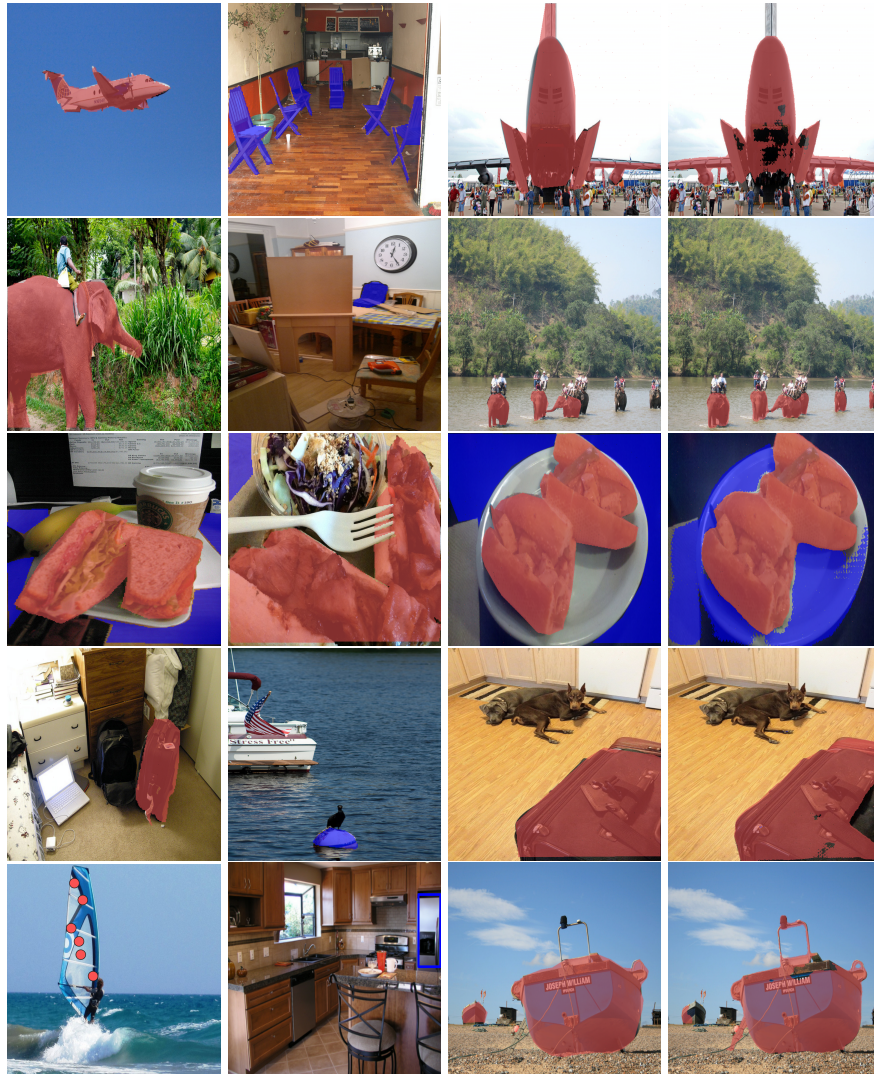
Furthermore, to validate the performances of LA in complex FSS settings, we tested our model capabilities also on an increasing  $N$  setting. Table 3 shows the results of LA and DCAMA on the  $N$ -way 1-shot segmentation task. Except for 1-way, LA outperforms DCAMA in all other  $N$ -way settings, showcasing its robustness and adaptability with a growing number of classes.

Figure 3 presents qualitative results from our 2-way 1-shot segmentation experiment on the COCO-20<sup>i</sup> dataset. This visual representation highlights the efficacy of our model in accurately interpreting and responding to diverse prompts, showcasing its robust segmentation capabilities in complex scenarios.

#### 4.4 Ablation Study

Our comprehensive ablation studies on the validation fold of COCO-20<sup>i</sup> dissected the contribution of each component within our model to its overall performance. We systematically omitted elements deemed non-critical—specifically, the Spatial Convolutions in the Mask Decoder, the Class Token Pool, and the Class Example Mixer from the Prompt Encoder—and observed the resultant impact on model efficacy. As delineated in Table 4, excluding the Spatial Convolutions from the Mask Decoder markedly diminished model performance. This component is pivotal for blending spatial details before classification, significantly enhancing segmentation quality. Meanwhile, the Class Token Pool and Class Example Mixer, though their removal slightly affected performance, were proven





**Fig. 3:** Visual representation of 2-way 1-shot segmentation on COCO-20<sup>i</sup>. Sequence from left to right includes the first prompt, the second prompt, the ground truth mask, and our model's prediction.

indispensable for optimizing results. These findings highlight the integral role of each component in achieving superior segmentation outcomes, underscoring the holistic synergy that drive our model's performance.

Our analysis also assessed the impact of different prompt types on our model's effectiveness, exploring how each type influences performance. Table 5 reveals that mask prompts led to the highest performance, offering the most detailed

Configuration	1-way 1-shot	2-way 1-shot
Complete model	39.2	30.9
w/o Spatial Convolutions	34.2	27.6
w/o Class Example Mixer	38.7	30.9
w/o Token Pool	38.3	30.1

**Table 4:** Ablation analysis on the COCO-20<sup>t</sup>'s fold-0 evaluating the impact of different components of the Label Anything architecture.

Prompt Type	1-way 1-shot	1-way 5-shot	2-way 1-shot	2-way 5-shot
Only masks	43.5	45.1	34.6	35.9
Boxes and points	37.1	40.8	29.2	30.7
Only boxes	38.3	41.2	30.6	31.5
Only points	36.5	39.9	29.0	29.4

**Table 5:** Ablation analysis evaluating the impact of different prompt types on model performance.

guidance for segmentation tasks. Nonetheless, the model demonstrated robust adaptability, yielding solid results even with alternative prompt types, albeit with a marginal reduction compared to masks alone. This underscores the model’s versatile capability to effectively manage and interpret various prompt types.

## 5 Conclusion

In this study, we presented Label Anything, an innovative framework for few-shot semantic segmentation that markedly advances the adaptability and efficiency of segmentation models. Our rigorous testing on the COCO-20<sup>t</sup> benchmark has showcased the model’s capacity to reach competitive and, in some instances, state-of-the-art performance, alongside its ability to generalize across diverse segmentation scenarios. Including a wide range of visual prompts—points, bounding boxes, and masks—empowers Label Anything to interpret and leverage multiple forms of input guidance effectively. The results highlight the efficacy of prototype-based approaches in addressing the challenges of multi-class FSS, presenting a compelling alternative to affinity-based methods which, despite their accuracy, struggle with scalability as the dataset expands.

We envision a broad spectrum of future research directions to advance our method. An intriguing avenue involves the integration of textual prompts, leveraging the interplay between textual and visual information to enrich the segmentation process. Concurrently, the proposal of an optimized example candidate selection mechanism, potentially through clustering approaches, promises to streamline the identification of example candidates within large-scale datasets, enhancing the efficiency of support set construction.

**Acknowledgement** We acknowledge the CINECA award under the ISCRA initiative, which gave us access to computing resources and support.

## References

1. Chen, H., Dong, Y., Lu, Z., Yu, Y., Han, J.: Pixel Matching Network for Cross-Domain Few-Shot Segmentation. In: Proceedings of the IEEE/CVF Winter Conference on Applications of Computer Vision. pp. 978–987 (2024)
2. Cheng, B., Misra, I., Schwing, A.G., Kirillov, A., Girdhar, R.: Masked-Attention Mask Transformer for Universal Image Segmentation. In: Proceedings of the IEEE/CVF Conference on Computer Vision and Pattern Recognition. pp. 1290–1299 (2022)
3. Çiçek, Ö., Abdulkadir, A., Lienkamp, S.S., Brox, T., Ronneberger, O.: 3D U-Net: Learning Dense Volumetric Segmentation from Sparse Annotation. In: Medical Image Computing and Computer-Assisted Intervention–MICCAI 2016: 19th International Conference, Athens, Greece, October 17–21, 2016, Proceedings, Part II 19. pp. 424–432. Springer (2016)
4. Dong, N., Xing, E.P.: Few-shot semantic segmentation with prototype learning. In: BMVC (2018)
5. Dosovitskiy, A., Beyer, L., Kolesnikov, A., Weissenborn, D., Zhai, X., Unterthiner, T., Dehghani, M., Minderer, M., Heigold, G., Gelly, S., et al.: An image is worth 16x16 words: Transformers for image recognition at scale. arXiv preprint arXiv:2010.11929 (2020)
6. Finn, C., Abbeel, P., Levine, S.: Model-Agnostic Meta-Learning for Fast Adaptation of Deep Networks (Jul 2017), arXiv:1703.03400 [cs]
7. Goyal, P., Dollár, P., Girshick, R., Noordhuis, P., Wesolowski, L., Kyrola, A., Tulloch, A., Jia, Y., He, K.: Accurate, large minibatch sgd: Training imagenet in 1 hour. arXiv preprint arXiv:1706.02677 (2017)
8. Kang, D., Cho, M.: Integrative few-shot learning for classification and segmentation. In: Proceedings of the IEEE/CVF Conference on Computer Vision and Pattern Recognition. pp. 9979–9990 (2022)
9. Kirillov, A., Mintun, E., Ravi, N., Mao, H., Rolland, C., Gustafson, L., Xiao, T., Whitehead, S., Berg, A.C., Lo, W.Y., et al.: Segment Anything. arXiv preprint arXiv:2304.02643 (2023)
10. Li, G., Jampani, V., Sevilla-Lara, L., Sun, D., Kim, J., Kim, J.: Adaptive prototype learning and allocation for few-shot segmentation. In: Proceedings of the IEEE/CVF conference on computer vision and pattern recognition. pp. 8334–8343 (2021)
11. Lin, T.Y., Goyal, P., Girshick, R., He, K., Dollár, P.: Focal loss for dense object detection. In: Proceedings of the IEEE international conference on computer vision. pp. 2980–2988 (2017)
12. Lin, T.Y., Maire, M., Belongie, S., Hays, J., Perona, P., Ramanan, D., Dollár, P., Zitnick, C.L.: Microsoft coco: Common objects in context. In: Computer Vision–ECCV 2014: 13th European Conference, Zurich, Switzerland, September 6–12, 2014, Proceedings, Part V 13. pp. 740–755. Springer (2014)
13. Liu, L., Cao, J., Liu, M., Guo, Y., Chen, Q., Tan, M.: Dynamic extension nets for few-shot semantic segmentation. In: Proceedings of the 28th ACM international conference on multimedia. pp. 1441–1449 (2020)
14. Liu, Y., Zhang, X., Zhang, S., He, X.: Part-aware prototype network for few-shot semantic segmentation. In: Computer Vision–ECCV 2020: 16th European Conference, Glasgow, UK, August 23–28, 2020, Proceedings, Part IX 16. pp. 142–158. Springer (2020)

15. Liu, Y., Liu, N., Yao, X., Han, J.: Intermediate prototype mining transformer for few-shot semantic segmentation. *Advances in Neural Information Processing Systems* **35**, 38020–38031 (2022)
16. Liu, Z., Lin, Y., Cao, Y., Hu, H., Wei, Y., Zhang, Z., Lin, S., Guo, B.: Swin transformer: Hierarchical vision transformer using shifted windows. In: *Proceedings of the IEEE/CVF international conference on computer vision*. pp. 10012–10022 (2021)
17. Long, J., Shelhamer, E., Darrell, T.: Fully Convolutional Networks for Semantic Segmentation. In: *Proceedings of the IEEE Conference on Computer Vision and Pattern Recognition*. pp. 3431–3440 (2015)
18. Loshchilov, I., Hutter, F.: Sgdr: Stochastic gradient descent with warm restarts. *arXiv preprint arXiv:1608.03983* (2016)
19. Loshchilov, I., Hutter, F.: Decoupled weight decay regularization. *arXiv preprint arXiv:1711.05101* (2017)
20. Mazurowski, M.A., Dong, H., Gu, H., Yang, J., Konz, N., Zhang, Y.: Segment Anything Model for Medical Image Analysis: An Experimental Study. *Medical Image Analysis* **89**, 102918 (2023)
21. Min, J., Kang, D., Cho, M.: Hypercorrelation squeeze for few-shot segmentation. In: *Proceedings of the IEEE/CVF international conference on computer vision*. pp. 6941–6952 (2021)
22. Nguyen, K., Todorovic, S.: Feature weighting and boosting for few-shot segmentation. In: *Proceedings of the IEEE/CVF International Conference on Computer Vision*. pp. 622–631 (2019)
23. Oktay, O., Schlemper, J., Folgoc, L.L., Lee, M., Heinrich, M., Misawa, K., Mori, K., McDonagh, S., Hammerla, N.Y., Kainz, B., et al.: Attention U-Net: Learning Where to Look for the Pancreas. *arXiv preprint arXiv:1804.03999* (2018)
24. Rakelly, K., Shelhamer, E., Darrell, T., Efros, A.A., Levine, S.: Conditional Networks for Few-Shot Semantic Segmentation. In: *International Conference on Learning Representations* (2018)
25. Ronneberger, O., Fischer, P., Brox, T.: U-Net: Convolutional Networks for Biomedical Image Segmentation. In: *Medical Image Computing and Computer-Assisted Intervention—MICCAI 2015: 18th International Conference, Munich, Germany, October 5–9, 2015, Proceedings, Part III 18*. pp. 234–241. Springer (2015)
26. Shaban, A., Bansal, S., Liu, Z., Essa, I., Boots, B.: One-Shot Learning for Semantic Segmentation. *British Machine Vision Conference (BMVC)* (2017)
27. Shi, X., Wei, D., Zhang, Y., Lu, D., Ning, M., Chen, J., Ma, K., Zheng, Y.: Dense cross-query-and-support attention weighted mask aggregation for few-shot segmentation. In: *European Conference on Computer Vision*. pp. 151–168. Springer (2022)
28. Snell, J., Swersky, K., Zemel, R.S.: Prototypical Networks for Few-shot Learning (Jun 2017), *arXiv:1703.05175 [cs, stat]*
29. Sung, F., Yang, Y., Zhang, L., Xiang, T., Torr, P.H.S., Hospedales, T.M.: Learning to Compare: Relation Network for Few-Shot Learning (Mar 2018), *arXiv:1711.06025 [cs]*
30. Tian, P., Wu, Z., Qi, L., Wang, L., Shi, Y., Gao, Y.: Differentiable meta-learning model for few-shot semantic segmentation. In: *Proceedings of the AAAI Conference on Artificial Intelligence*. pp. 12087–12094 (2020)
31. Tian, Z., Zhao, H., Shu, M., Yang, Z., Li, R., Jia, J.: Prior guided feature enrichment network for few-shot segmentation. *IEEE transactions on pattern analysis and machine intelligence* **44**(2), 1050–1065 (2020)
32. Vinyals, O., Blundell, C., Lillicrap, T., Kavukcuoglu, K., Wierstra, D.: Matching Networks for One Shot Learning (Dec 2017), *arXiv:1606.04080 [cs, stat]*

33. Wang, K., Liew, J.H., Zou, Y., Zhou, D., Feng, J.: Panet: Few-shot image semantic segmentation with prototype alignment. In: proceedings of the IEEE/CVF international conference on computer vision. pp. 9197–9206 (2019)
34. Wang, X., Zhang, X., Cao, Y., Wang, W., Shen, C., Huang, T.: SegGPT: Segmenting Everything In Context. arXiv e-prints pp. arXiv-2304 (2023)
35. Wang, Y., Sun, R., Zhang, T.: Rethinking the Correlation in Few-Shot Segmentation: A Buoy's View. In: Proceedings of the IEEE/CVF Conference on Computer Vision and Pattern Recognition. pp. 7183–7192 (2023)
36. Xie, D., Wang, R., Ma, J., Chen, C., Lu, H., Yang, D., Shi, F., Lin, X.: Edit Everything: A Text-Guided Generative System for Images Editing. arXiv preprint arXiv:2304.14006 (2023)
37. Yu, T., Feng, R., Feng, R., Liu, J., Jin, X., Zeng, W., Chen, Z.: Inpaint Anything: Segment Anything Meets Image Inpainting. arXiv preprint arXiv:2304.06790 (2023)
38. Zhang, B., Xiao, J., Qin, T.: Self-guided and cross-guided learning for few-shot segmentation. In: Proceedings of the IEEE/CVF Conference on Computer Vision and Pattern Recognition. pp. 8312–8321 (2021)
39. Zhang, C., Lin, G., Liu, F., Yao, R., Shen, C.: Canet: Class-agnostic segmentation networks with iterative refinement and attentive few-shot learning. In: Proceedings of the IEEE/CVF conference on computer vision and pattern recognition. pp. 5217–5226 (2019)
40. Zhang, G., Kang, G., Yang, Y., Wei, Y.: Few-shot segmentation via cycle-consistent transformer. *Advances in Neural Information Processing Systems* **34**, 21984–21996 (2021)
41. Zhang, J.W., Sun, Y., Yang, Y., Chen, W.: Feature-proxy transformer for few-shot segmentation. *Advances in Neural Information Processing Systems* **35**, 6575–6588 (2022)
42. Zhang, M., Shi, M., Li, L.: MFNet: Multiclass Few-Shot Segmentation Network With Pixel-Wise Metric Learning. *IEEE Transactions on Circuits and Systems for Video Technology* **32**(12), 8586–8598 (2022)
43. Zhang, X., Wei, Y., Yang, Y., Huang, T.S.: Sg-one: Similarity guidance network for one-shot semantic segmentation. *IEEE transactions on cybernetics* **50**(9), 3855–3865 (2020)
44. Zou, X., Yang, J., Zhang, H., Li, F., Li, L., Wang, J., Wang, L., Gao, J., Lee, Y.J.: Segment everything everywhere all at once. *Advances in Neural Information Processing Systems* **36** (2024)